NEOPLASIA
www.neoplasia.com

Volume 15 Number 7 July 2013 pp. 815–825 815

Inhibition of Tumor Angiogenesis and Tumor Growth by the DSL Domain of Human Delta-Like 1 Targeted to Vascular Endothelial Cells[1,2]

Xing-Cheng Zhao[3], Guo-Rui Dou[3], Li Wang[3], Liang Liang, Deng-Mei Tian, Xiu-Li Cao, Hong-Yan Qin, Chun-Mei Wang, Ping Zhang and Hua Han

State Key Laboratory of Cancer Biology, Department of Medical Genetics and Developmental Biology, Fourth Military Medical University, Xi'an, China

Abstract

The growth of solid tumors depends on neovascularization. Several therapies targeting tumor angiogenesis have been developed. However, poor response in some tumors and emerging resistance necessitate further investigations of new drug targets. Notch signal pathway plays a pivotal role in vascular development and tumor angiogenesis. Either blockade or forced activation of this pathway can inhibit angiogenesis. As blocking Notch pathway results in the formation of vascular neoplasm, activation of Notch pathway to prevent tumor angiogenesis might be an alternative choice. However, an *in vivo* deliverable reagent with highly efficient Notch-activating capacity has not been developed. Here, we generated a polypeptide, hD1R, which consists of the Delta–Serrate–Lag-2 fragment of the human Notch ligand Delta-like 1 and an arginine-glycine-aspartate (RGD) motif targeting endothelial cells (ECs). We showed that hD1R could bind to ECs specifically through its RGD motif and effectively triggered Notch signaling in ECs. We demonstrated both *in vitro* and *in vivo* that hD1R inhibited angiogenic sprouting and EC proliferation. In tumor-bearing mice, the injection of hD1R effectively repressed tumor growth, most likely through increasing tumor hypoxia and tissue necrosis. The amount and width of vessels reduced remarkably in tumors of mice treated with hD1R. Moreover, vessels in tumors of mice treated with hD1R recruited more $NG2^+$ perivascular cells and were better perfused. Combined application of hD1R and chemotherapy with cisplatin and teniposide revealed that these two treatments had additive antitumor effects. Our study provided a new strategy for antiangiogenic tumor therapy.

Neoplasia (2013) 15, 815–825

Introduction

It has been recognized for decades that solid tumors require neovascularization essentially through angiogenesis [1,2]. Tumor cells and other microenvironmental cells secrete angiogenic factors such as vascular endothelial growth factor (VEGF) and platelet-derived growth factor, which cooperate with other molecules to fulfill angiogenesis in tumors. Therapies targeting tumor angiogenic factors have been developed [3–7], but poor responses in some tumors and emerging resistance have prompted further investigations of new drug targets and strategies [8–10].

The Notch signal pathway plays a pivotal role in physiological vascular development [11–16] and tumor angiogenesis [15,17–22]. In mammals, the canonical Notch pathway is composed of five Notch ligands [Delta-like (Dll) 1, 3, 4, Jagged 1, 2], four Notch receptors (Notch1–4), the transcription factor RBP-J, and the downstream

Abbreviations: Dll1, Delta-like 1; ECs, endothelial cells; HUVECs, human umbilical vein endothelial cells; RGD, arginine-glycine-aspartate; NICD, intracellular domain of Notch receptors

Address all correspondence to: Hua Han, PhD, Department of Medical Genetics and Developmental Biology, Fourth Military Medical University, Xi'an 710032, China. E-mail: huahan@fmmu.edu.cn or Ping Zhang, PhD, Department of Medical Genetics and Developmental Biology, Fourth Military Medical University, Xi'an 710032, China. E-mail: pingzhang0622@gmail.com

[1]This work was supported by grants from the Ministry of Science and Technology (2009CB521706, 2011ZXJ09101-02C, 2009ZX09301-009-RC11, and CWS11J143) and the Natural Science Foundation of China (30830067, 31130019, and 91029731). No potential conflicts of interest were disclosed.

[2]This article refers to supplementary materials, which are designated by Table W1 and Figures W1 to W9 and are available online at www.neoplasia.com.

[3]Equal contributors.

Received 26 February 2013; Revised 19 April 2013; Accepted 22 April 2013

DOI 10.1593/neo.13550

effectors such as the Hes family molecules [11]. The Notch ligand–receptor interaction mediated by the Delta–Serrate–Lag-2 (DSL) domains of the ligands triggers serial proteolytic cleavages of receptors, which release the intracellular domain of Notch receptors (NICD). NICD further associates with RBP-J and transactivates downstream genes involved in multiple steps of angiogenesis including sprouting, extension, and maturation of neovasculature [11,12,17].

Blocking Notch signal inhibits tumor growth through nonproductive angiogenesis [20–24], but this treatment results in the formation of vascular neoplasms [25]. Activating Notch pathway may be an alternative way to modulate angiogenesis because forced activation of endothelial Notch signaling also inhibits angiogenesis [19,26–29]. However, although a soluble DSL domain of Dll1 is sufficient for triggering Notch signal *in vitro*, it might be inefficient or even inhibitory to Notch signal activation *in vivo*, because of their incompetence in inducing endocytosis of Notch ligands on the signal-sending cells, a necessary step for Notch activation [30,31]. To produce a soluble Notch ligand with a better capability to induce endocytosis *in vivo*, we designed a fusion protein, hD1R, which is composed of the DSL domain of the human (h)Dll1 (amino acids 127–225) and an arginine-glycine-aspartate (RGD)–containing nonapeptide (CRGDCGVRY). RGD targets the integrin αvβ3 expressed on endothelial cells (ECs) in response to angiogenic growth factors and tumors [32–34] and it has been shown that the binding of RGD-containing molecular ligands with cell surface integrins triggers endocytosis [35]. In this study, we demonstrated that hD1R can effectively trigger Notch signaling in ECs and inhibit angiogenesis and tumor growth, thus providing a novel strategy for antiangiogenic tumor therapy.

Materials and Methods

Expression of Recombinant Proteins in Escherichia coli

The cDNA fragment encoding the DSL domain of hDll1 (NM_005618) was amplified by using polymerase chain reaction (PCR) from a human cDNA library. The product was fused with an RGD motif (hD1R) or a DGR motif (hD1D) by PCR. The PCR primers are listed in Table W1. The resultant gene fragments were cloned into pET32a(+) between the *Nco*I and *Xho*I sites to construct pET32a-hD1S (stop), pET32a-hD1R (RGD fusion), and pET32a-hD1D (DGR fusion), respectively (Figure 1*A*). For the production of the recombinant proteins, *E. coli* BL21 was transformed with the plasmids. Positive clones were expanded in Luria-Bertani medium, and cells at the exponential stage were induced with 0.5 mM isopropyl β-D-thiogalactoside. The Trx-hD1S, Trx-hD1R, and Trx-hD1D proteins were purified by using Ni^{2+}-NTA columns (Invitrogen, Carlsbad, CA) according to the manufacturer's manuals. To obtain the S-tagged hD1S, hD1R, and hD1D proteins, Trx-hD1S, Trx-hD1R, and Trx-hD1D were cleaved by using thrombin (Novagen, Darmstadt, Germany) and further purified by using Ni^{2+}-NTA columns following the supplier's instructions. For Western blot, proteins were separated by sodium dodecyl sulfate–polyacrylamide gel electrophoresis (SDS-PAGE) and electroblotted onto polyvinylidene difluoride (PVDF) membrane. Membranes were probed by using anti-His (Sigma, St Louis, MO) or anti–S-Tag antibody (Novagen) at appropriate dilutions, followed by incubation with an HRP-conjugated secondary anti-mouse IgG antibody (Millipore, Billerica, MA). Blots were developed by using the enhanced chemiluminescence system (Clinx Science Instruments, Shanghai, China).

Cell Culture

The tumor cell lines U87, LLC, and MCF-7 (ATCC, Manassas, VA) were maintained in RPMI 1640 medium (Invitrogen) supplemented with 10% FBS, 2 mM L-glutamine, 100 IU/ml penicillin, and 100 μg/ml streptomycin sulfate. Human umbilical vein ECs (HUVECs) were cultured in the endothelial cells media (ECM; ScienCell, San Diego, CA) supplemented with 10% FBS, 100 IU/ml penicillin, 100 μg/ml streptomycin, and endothelial cell growth supplement (ECGS; ScienCell). The recombinant hD1S, hD1D, or hD1R was added at the concentration of 1 μg/ml. γ-Secretase inhibitor (GSI; DAPT; Alexis Biochemicals, San Diego, CA) and Dynasore (Sigma) were used at the concentration of 75 and 40 μM, respectively. For the cell adhesion assay, wells of 96-well dishes were coated with 100 μl of different recombinant proteins (50 μg/ml) overnight, and then 1×10^5 HUVECs were seeded in each well. In some cases, an RGD peptide (CRGDCGVRY) or a DGR peptide (CDGRCGVRY; CL Bio-Scientific, Xi'an, China) was included at the concentration of 1 μg/ml. Cells were cultured for 1.5 hours, and nonadhesive cells were discarded by rinsing with phosphate-buffered saline (PBS). Adherent cells were stained with crystal violet, photographed, and quantified by light absorbance at A620 using a spectrometer.

Flow Cytometry

For flow cytometry, single-cell suspensions were prepared from cultured cells or mouse lymphoid tissues and stained with appropriate antibodies. Then, cells were analyzed by using a FACSCalibur flow cytometer (BD Immunocytometry Systems, San Jose, CA) and the CellQuest software. Dead cells were excluded using propidium iodide staining. S-Tag was stained with a rabbit anti–S-Tag antibody followed by fluorescein isothiocyanate–conjugated goat anti-rabbit IgG (Santa Cruz Biotechnology, Inc, Santa Cruz, CA). Other antibodies used for staining were given as follows: anti-CD19 (1D3; BD Pharmingen, San Jose, CA), anti-CD21 (7G6; Biolegend, San Diego, CA), anti-CD23 (B3B4; Biolegend), anti-CD3 (145-2C11; Biolegend), anti-CD4 (RM4-5; BD Pharmingen), and anti-CD8 (53-6.7; BD Pharmingen).

Quantitative Reverse Transcription–PCR

Total RNA was extracted by using the TRIzol reagent (Invitrogen) according to the manufacturer's instructions. cDNA was prepared by using a reverse transcription (RT) system (Takara Dalian, Dalian, China). Quantitative real-time PCR was performed in triplicates by using a kit (SYBR Premix EX Taq; Takara) and the ABI PRISM 7500 Real-Time PCR System, with β-actin as an internal control. The PCR primers are listed in Table W1.

Fibrin Bead Assay

HUVECs were tested for angiogenic sprouting with the fibrin bead assay using a kit (Amersham Pharmacia Biotech, Piscataway, NJ) according the supplier's instructions [36]. Briefly, HUVECs were cultured in EGM-2 medium (Clonetics, Walkersville, MD) the day before beading. Cytodex 3 microcarrier beads (Amersham) were prepared according to the supplier's instructions, and the beads were incubated with HUVECs (400 cells per bead) at 37°C for 4 hours. The coated beads were transferred to a tissue culture flask (T25; Falcon, Bedford, MA) and left overnight in 5 ml of EGM-2 at 37°C and 5% CO_2. The beads were washed three times and were suspended at a density of 500 beads/ml in the fibrinogen solution with 0.625 U/ml thrombin, and the fibrinogen/bead suspension (0.5 ml) was distributed in each well of a 24-well plate. After clotting at room temperature for 5 minutes and then at 37°C and 5% CO_2/95% air for 15 minutes,

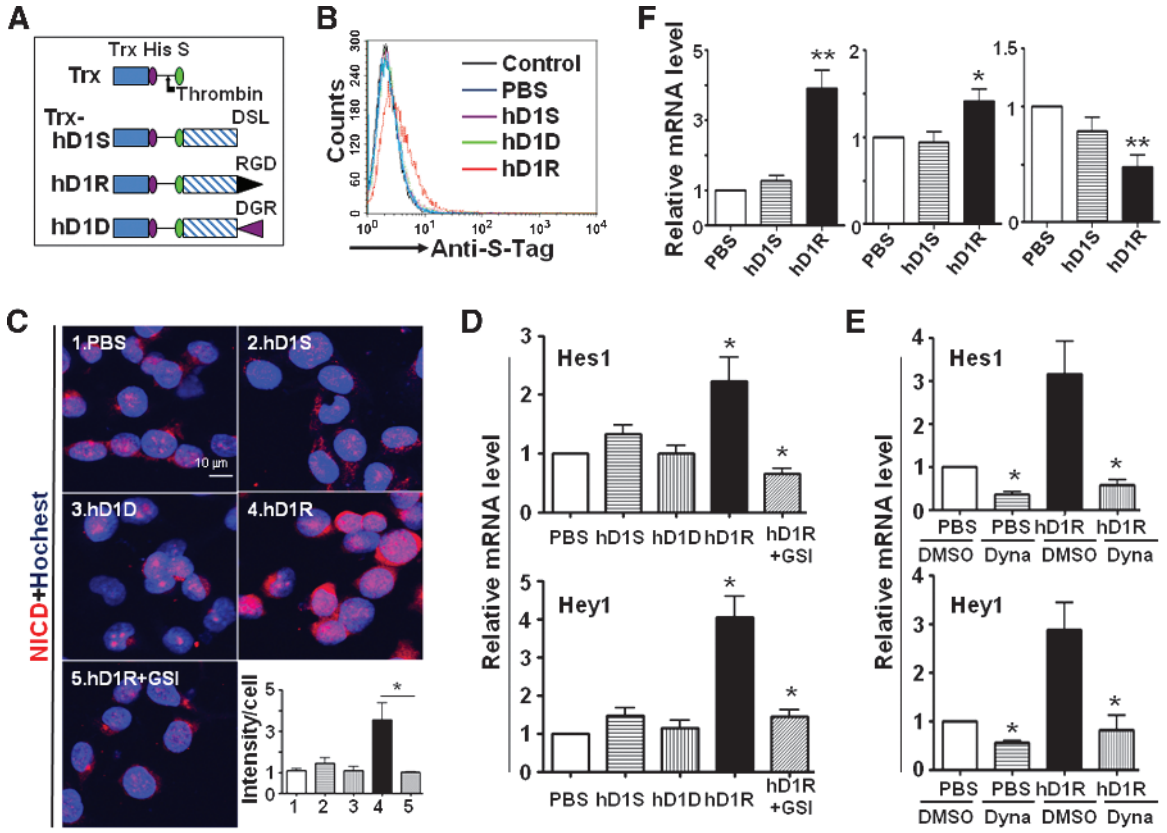

Figure 1. EC-targeted hDll1 efficiently activated Notch signaling. (A) Schematic representatives of recombinant proteins. Trx, His, S, DSL, RGD, and DGR indicate thioredoxin, His tag, S tag, DSL domain of hDll1, RGD peptide, and DGR peptide, respectively. The site of thrombin cleavage is indicated with an arrow. (B) HUVECs were incubated with PBS, hD1S, hD1R, or hD1D and examined by FACS after secondary staining with anti–S-Tag. (C) hD1R activates Notch signaling in RGD- and GSI-dependent ways. HUVECs were incubated with PBS, hD1S, hD1R, or hD1D for 24 hours. GSI was included in some of the cultures as indicated. Cells were stained by immunofluorescence using anti-NICD. The intensity of fluorescent signals per cell was quantified and shown in the inset. (D) HUVECs were treated as in C. Cells were harvested and the expressions of Hes1 and Hey1 were detected by quantitative RT-PCR. (E) Activation of Notch signaling by hD1R required endocytosis. HUVECs were incubated with PBS or hD1R for 24 hours. DMSO or Dynasore was included in the medium as indicated. The expression of Hes1 and Hey1 was detected by using quantitative RT-PCR. (F) Activation of endothelial Notch signaling by hD1R *in vivo*. P3 pups were injected daily s.c. with PBS, hD1S, or hD1R. On P7, the retinas of the pups were collected and used for real-time RT-PCR for the expression of Hes1, VEGFR1, and VEGFR2, with CD31 as a reference control. Bars, means ± SD. $*P < .05$, $**P < .01$, $n = 5$.

EGM-2 (1 ml) was added to each well slowly and lung fibroblasts were seeded on top of the clot at a concentration of 20,000 cells/well. PBS, hD1R, DMSO, or GSI was included depending on the experiments. Images of the beads were captured by using an inverted microscope (CKX41; Olympus, Tokyo, Japan) with a charge-coupled device (CCD) camera (DP70; Olympus), and the number and length of the sprouts were measured.

Endothelial Network Formation Assay

Matrigel Basement Membrane Matrix (BD Biosciences) was thawed overnight at 4°C and diluted with medium to coat wells of 48-well dishes at 37°C for 30 minutes. HUVECs (1×10^5) were seeded on the gel in 400 μl of medium and incubated at 37°C and 5% CO_2 for 3 hours. hD1S or hD1R was added simultaneously when the cells were seeded at the concentration of 1 μg/ml. Images were captured by using a converted microscope with a CCD camera. The network formation was quantified by counting branches and the length of the enclosed lumens.

Tumor-bearing Mouse Models. Tumor cells (5×10^6) were injected subcutaneously (s.c.) into nude mice brought about under specific pathogen–free conditions. PBS or hD1R (80 μg/injection) was injected intraperitoneally (i.p.) twice per week from the 7th day of the tumor inoculation. In some cases, cisplatin or teniposide were administrated i.p. at the concentration of 5 mg/kg once a week. Tumor growth was monitored by measuring the tumor length (L) and short (S) with a sliding caliper from the 7th day of tumor inoculation (tumor size = $L \times S^2 \times 0.51$). On the ending day of the experiment, the body weights of the mice were recorded before being sacrificed. Tumors were removed, weighed, and used for further histologic examinations. Tumor weight index was calculated as the ratio of tumor weight *versus* body weight. All animal experiments were approved by the Animal Experiment Administration Committee of the university.

Histology

Tissues were fixed by immersing in 4% paraformaldehyde for 2 hours at 4°C, followed by immersing in 25% sucrose in PBS overnight. The samples were embedded in optimal cutting temperature (OCT)

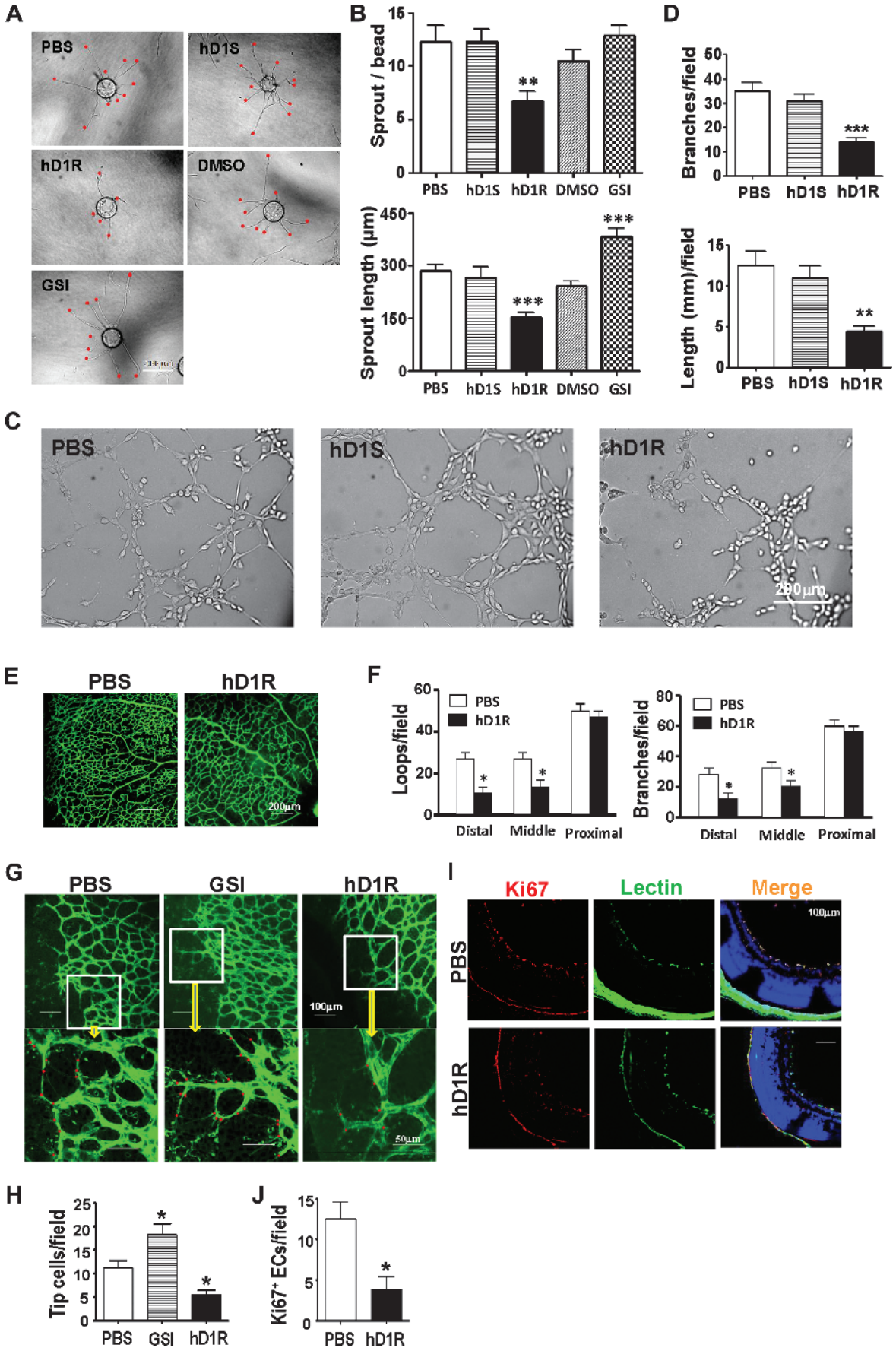
A
PBS
hD1S
hD1R
DMSO
GSI
B
Sprout / bead
PBS hD1S hD1R DMSO GSI
Sprout length (μm)
PBS hD1S hD1R DMSO GSI
D
Branches/field
PBS hD1S hD1R
Length (mm)/field
PBS hD1S hD1R
C
PBS
hD1S
hD1R
200μm
E
PBS
hD1R
200μm
F
Loops/field
PBS
hD1R
Distal Middle Proximal
Branches/field
PBS
hD1R
Distal Middle Proximal
G
PBS
GSI
hD1R
100μm
50μm
I
Ki67
Lectin
Merge
PBS
hD1R
100μm
H
Tip cells/field
PBS GSI hD1R
J
Ki67+ ECs/field
PBS hD1R

compound (Sakura Finetek, Inc, Torrance, CA), sectioned at 10-μm thickness, and then dried at room temperature for 2 hours. Hematoxylin and eosin (H&E) staining was performed according to routine protocols.

For immunofluorescence staining, cryosections were blocked with 1% BSA in PBS and then incubated with rat anti-CD31 (Biolegend), rabbit anti–S-Tag (Abcam, Cambridge, MA), rabbit anti-NG2 (Millipore), or rabbit anti-Ki67 (Thermo Scientific, Fremont, CA) as the primary antibodies. After washing, sections were incubated with secondary antibodies including biotinylated goat anti-rat secondary antibody (Vector Laboratories, Burlingame, CA), Cy3-conjugated goat anti-rabbit IgG (Sigma), or fluorescein isothiocyanate–conjugated goat anti-mouse IgG (Sigma). In some cases, Cy3-conjugated streptavidin (Sigma) or DyLight 488 streptavidin (Vector Laboratories) was applied. Images were acquired under a fluorescence microscope (BX51; Olympus) or a confocal microscope (FV1000; Olympus). Cultured cells were stained in a similar way by using rabbit anti–S-Tag or rabbit anti-NICD (Abcam), followed by Cy3-conjugated goat anti-rabbit IgG (Sigma), and observed under a microscope.

For whole-mount staining of retinal vasculature, postnatal day 3 (P3) pups were injected s.c. with PBS, GSI, or hD1R (25 μg) once a day. Retinas were collected on P7, flat-mounted, and fixed in 4% paraformaldehyde for 2 hours. The samples were permeabilized with 0.2% Triton X-100 for 2 hours and then stained with fluorescein-labeled *Griffonia simplicifolia* Lectin I (Vector Laboratories) for 24 hours at 4°C. After washing, images were taken under a fluorescence microscope or a confocal microscope.

To visualize hypoxic regions in tumors, pimonidazole HCl (60 mg/kg; Hypoxyprobe Inc, Burlington, MA) was injected i.p. into mice 1 hour before sacrifice. Anesthetized mice were then perfused with 4% paraformaldehyde solution in 0.1 M phosphate buffer (pH 7.2). Tumors were sectioned and stained by using rabbit anti-Hypoxyprobe (PIMO) antibody (Hypoxyprobe Inc) and Cy3-conjugated goat anti-rabbit (Sigma). To detect perfused blood vessels, a biotinylated lectin (*Lycopersicon esculentum*, 100 μg; Vector Laboratories) was injected intravenously through the tail veins, and the mice were sacrificed 30 minutes later. Tumors were subsequently fixed by perfusion with paraformaldehyde solution as above.

Sample preparation and observation with scanning electron microscope (SEM) were as described [37].

Statistics

Pixels for each color were calculated by using Image Pro Plus 6.0 software to quantitatively represent the intensity of positive cells. Statistical analysis was performed with the SPSS 12.0 program. Comparisons between groups were undertaken using unpaired Student's *t* test. Results were expressed as means ± SD. $P < .05$ was considered statistically significant.

Results

hD1R Efficiently Bound to ECs

Recombinant Trx-hD1R was manufactured in *E. coli* and purified by using Ni^{2+}-NTA columns. The product was cleaved with thrombin followed by affinity chromatography to obtain hD1R with an S-Tag at the N terminus (Figures 1*A* and W1). hD1S (the DSL domain of hDll1 with a stop codon at the C terminus) and hD1D (the DSL domain of hDll1 fused with a DGR-containing nonapeptide, CDGRCGVRY) were produced as well and employed as controls.

To evaluate the binding activity of hD1R with ECs, HUVECs were incubated with PBS, hD1S, hD1D, or hD1R and then subjected to indirect immunofluorescent staining with an anti–S-Tag antibody, followed by fluorescence-activated cell sorting (FACS) analysis. The result showed that hD1R but not hD1S or hD1D could bind to HUVECs (Figure 1*B*). This was confirmed by the observation that displayed significant staining of HUVECs incubated with hD1R but not hD1S or hD1D under a fluorescence microscope (Figure W2). Moreover, in a cell adhesion assay, we found that more HUVECs adhered to culture dishes precoated with hD1R than to dishes precoated with hD1S or hD1D. The adherence of HUVECs to hD1R-coated dishes could be blocked by a synthetic RGD nonapeptide but not by a DGR nonapeptide (Figure W3). These results demonstrated that hD1R could efficiently bind to HUVECs, most likely through the RGD motif. In addition, co-immunoprecipitation assay also showed that hD1R could interact with the extracellular domain of Notch1 (Figure W4).

Activation of Endothelial Notch Signaling by hD1R

In HUVECs incubated with hD1R, immunofluorescence staining and Western blot analysis showed an increase in the level of NICD, which was abrogated by GSI (Figures 1*C* and W5). In contrast, neither hD1S nor hD1D enhanced NICD level in HUVECs. Consistently, the mRNA level of Hes1 and Hey1, two major Notch downstream targets in ECs, increased remarkably in a γ-secretase–dependent way in hD1R-treated, but not hD1S- or hD1D-treated, HUVECs (Figure 1*D*). Interestingly, the hD1R-induced Notch activation in HUVECs was blocked by the dynamin inhibitor Dynasore (Figure 1*E*), consistent with the assumption that the RGD motif of hD1R most likely mediated the endocytosis of hD1R, which is essential for efficient Notch

Figure 2. hD1R repressed angiogenesis both *in vitro* and *in vivo*. (A, B) HUVECs were mixed with Cytodex 3 microbeads (400 cells per bead) and cultured for 24 hours for angiogenic sprouting in the presence of PBS, hD1R, hD1S, DMSO, or GSI. Each sprout was labeled with a red dot (A) and the numbers of sprouts and the sprout length per bead were counted and compared (B). (C, D) HUVECs were cultured in 48-well dishes coated with Matrigel Basement Membrane Matrix in the presence of PBS, hD1S, or hD1R. Cells were cultured under the indicated conditions for 3 hours and photographed under a microscope (C). The formation of endothelial networks was quantified by counting branch points and length of cells along the lumens (D) and compared. (E, F) P3 pups were injected daily s.c. with PBS or hD1R. On P7, the retinas of the pups were collected, flat-mounted, and stained with fluorescein-labeled *Griffonia simplicifolia* Lectin I. The structures of the whole retinal vasculature were shown (E). The numbers of enclosed capillary loops and vessel branch points were compared (F). (G, H) P3 pups were injected daily s.c. with PBS, GSI, or hD1R. On P7, the retinas of the pups were collected, flat-mounted, and stained with fluorescein-labeled *Griffonia simplicifolia* Lectin I. Tip cells at the angiogenic fronts were counted (G) and compared (H). (I, J) P3 pups were injected daily s.c. with PBS or hD1R. On P7, the retinas of the pups were collected and sectioned. The samples were co-stained with anti-Ki67 (red) and lectin (green) and were counterstained with Hoechst (I). The $Ki67^+$ signals were compared (J). Bars, means ± SD. $^*P < .05$, $^{**}P < .01$, $^{***}P < .001$, $n = 5$.

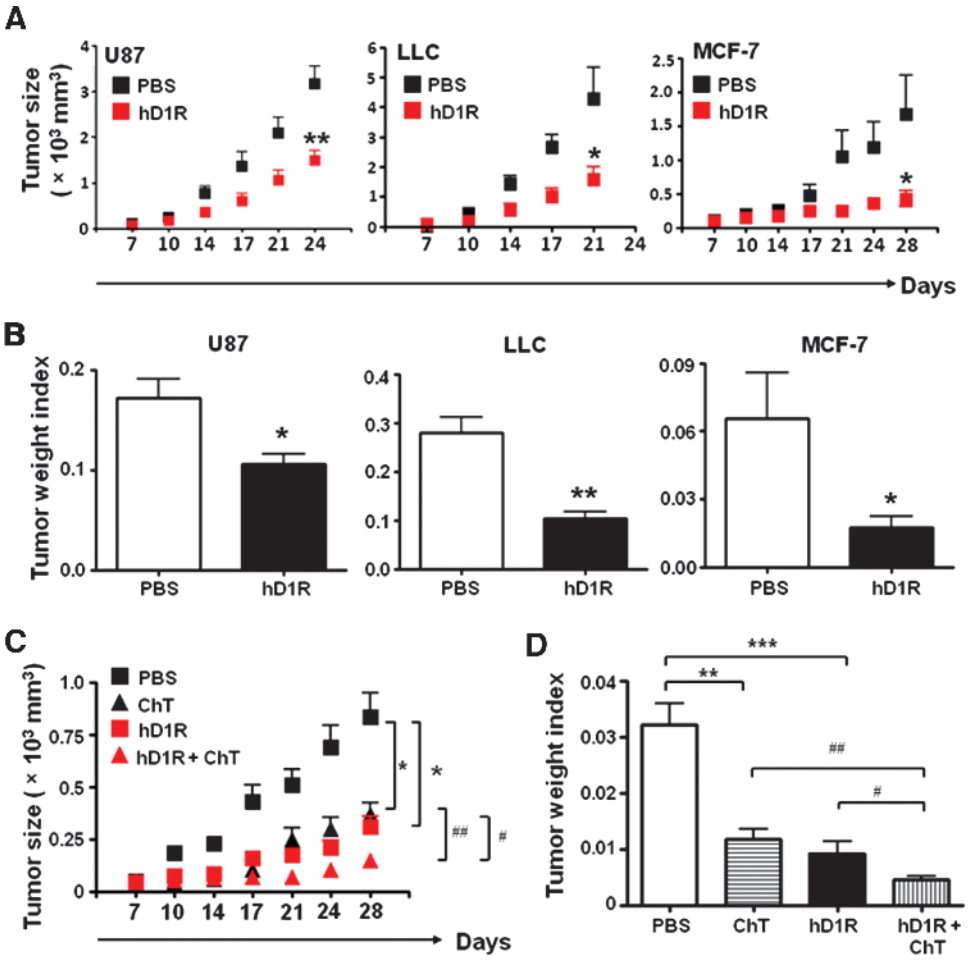

Figure 3. hD1R inhibited tumor growth. (A) U87, LLC, and MCF-7 cells were inoculated s.c. in nude mice. The mice were injected i.p. with PBS or hD1R twice a week from the 7th day of the tumor inoculation. The growth of tumors was monitored by measuring tumor size twice a week from the 7th day after tumor cell inoculation. (B) Tumors were dissected on the last day of the experiments, and tumor weight indexes were calculated and compared. (C) MCF-7 cells were inoculated s.c. in nude mice. The mice were injected i.p. with PBS, ChT, hD1R, or hD1R plus ChT from the 7th day of the tumor inoculation. The growth of tumors was monitored by measuring tumor size twice a week from the 7th day after tumor cell inoculation. (D) Tumors were dissected on the last day of the experiments, and tumor weight indexes were calculated and compared. Bars, means ± SD. $^{*,\#}P < .05$, $^{**,\#\#}P < .01$, $^{***}P < .001$, $n = 8$.

activation [30,31]. To evaluate the ability of hD1R to activate Notch signaling *in vivo*, purified hD1R was injected s.c. into P3 pups. The developing retinal vasculature was isolated on P7, and the expressions of Hes1, VEGF receptor 1 (VEGFR1), and VEGFR2 were assessed with quantitative RT-PCR. The results showed that the treatment with hD1R significantly elevated the expression of Hes1 and VEGFR1 while reduced the expression of VEGFR2, in line with Notch activation in ECs (Figure 1*F*). These results suggested that hD1R could efficiently activate Notch signaling in ECs.

hD1R Repressed Angiogenesis In Vitro *and* In Vivo

We then employed *in vitro* assays to examine the effects of hD1R on angiogenic sprouting and lumen formation by ECs. A fibrin gel bead assay was established with HUVECs in the presence of PBS, hD1R, hD1S, DMSO, or GSI, and the numbers of sprouts on each bead were counted. The result showed that hD1R significantly reduced the number and the length of the sprouts under the sprouting condition (Figure 2, *A* and *B*). Moreover, HUVECs were cultured in a Matrigel Basement Membrane Matrix in the presence of PBS, hD1S, or hD1R, and the formation of endothelial networks was compared by counting network branches and lengths. The result showed that hD1R dramatically inhibited network formation by HUVECs (Figure 2, *C* and *D*). Collectively, these data suggested that hD1R repressed angiogenesis *in vitro*.

We next examined the effects of hD1R on retinal angiogenesis. Pups were injected daily s.c. with PBS or hD1R from P3, and the angiogenic sprouting of retinal vasculature was examined on P7 by whole-mount retinal staining with lectin. The comparison of the number of capillary-enclosed loops and the number of vessel branch points indicated that the administration of hD1R significantly reduced the density of retinal vasculature in the distal and middle areas compared with the control. The vessel density in the proximal areas of retinal vasculature appeared not to be affected by hD1R administration, in line with the fact that angiogenesis had been completed in these areas (Figures 2, *E* and *F*, and W6). In addition, as shown in Figure 2, *G* and *H*, consistent with the *in vitro* observations, hD1R reduced while GSI increased the number of tip cells at the angiogenic fronts. Furthermore, to inspect the effects of hD1R on endothelial proliferation, we injected P3 pups s.c.

with PBS or hD1R and observed the proliferation of retinal ECs on P7 by immunofluorescent staining of the Ki67 antigen on lectin-marked ECs in retinal sections. The result showed that the numbers of $Ki67^+$ ECs decreased remarkably in retinas of pups injected with hD1R (Figure 2, *I* and *J*). These *in vivo* data demonstrated that hD1R inhibited angiogenesis, most likely by suppressing the formation of tip cells and EC proliferation.

hD1R Repressed Tumor Growth

We investigated the effects of hD1R on tumor growth. In a preliminary experiment, U87 human glioma cells were inoculated s.c. in nude mice. PBS or different dosage (20, 40, 60, and 80 μg/injection) of hD1R was injected i.p. every 2 days from the 7th day of tumor inoculation up to the 16th day. Observation of tumor growth showed that injection of hD1R dose-dependently repressed tumor growth (data not shown). We then examined the effect of hD1R on the growth of the U87 and LLC mouse lung cancer cells and the MCF-7 human breast cancer cells. Tumor cells (5×10^6) were inoculated s.c. in nude mice. Seven days after the initial inoculation, when tumor sizes were about 0.05×10^3 mm^3, PBS or hD1R was injected i.p. into tumor-bearing nude mice. As shown in Figure 3*A*, in all three types of tumors, hD1R significantly repressed tumor growth compared with the control group. At the end of the experiment when the tumors were collected, measurement of tumor weight index also indicated that hD1R significantly repressed tumor growth (Figure 3*B*).

To further evaluate the therapeutic efficacy of hD1R in combination with chemotherapy, MCF7 cells were inoculated s.c. in nude mice, and the mice were treated with PBS, cisplatin and teniposide (ChT), hD1R, or hD1R plus ChT from the 7th day of tumor inoculation up to 28th day. Tumor growth was monitored twice a week, and at the end of the experiment, tumors were collected and assessed for tumor weight index. The result showed that, while hD1R or ChT treatment could dramatically reduce tumor growth comparably, combined application of hD1R and ChT further decreased tumor size significantly compared with the monotreatments (Figure 3*C*). This observation was further supported by tumor weight index analysis (Figure 3*D*). These results suggested that hD1R could repress tumor growth, and hD1R and ChT had additive effects in suppressing tumors when used together.

Application of hD1R Enhanced Tumor Hypoxia

Histologic examination of tumor tissues by H&E staining showed that the application of hD1R induced more severe necrosis in tumors (Figure 4, *A* and *B*). We also assessed hypoxia in the tumor tissues by PIMO perfusion followed by anti-PIMO staining, and the result

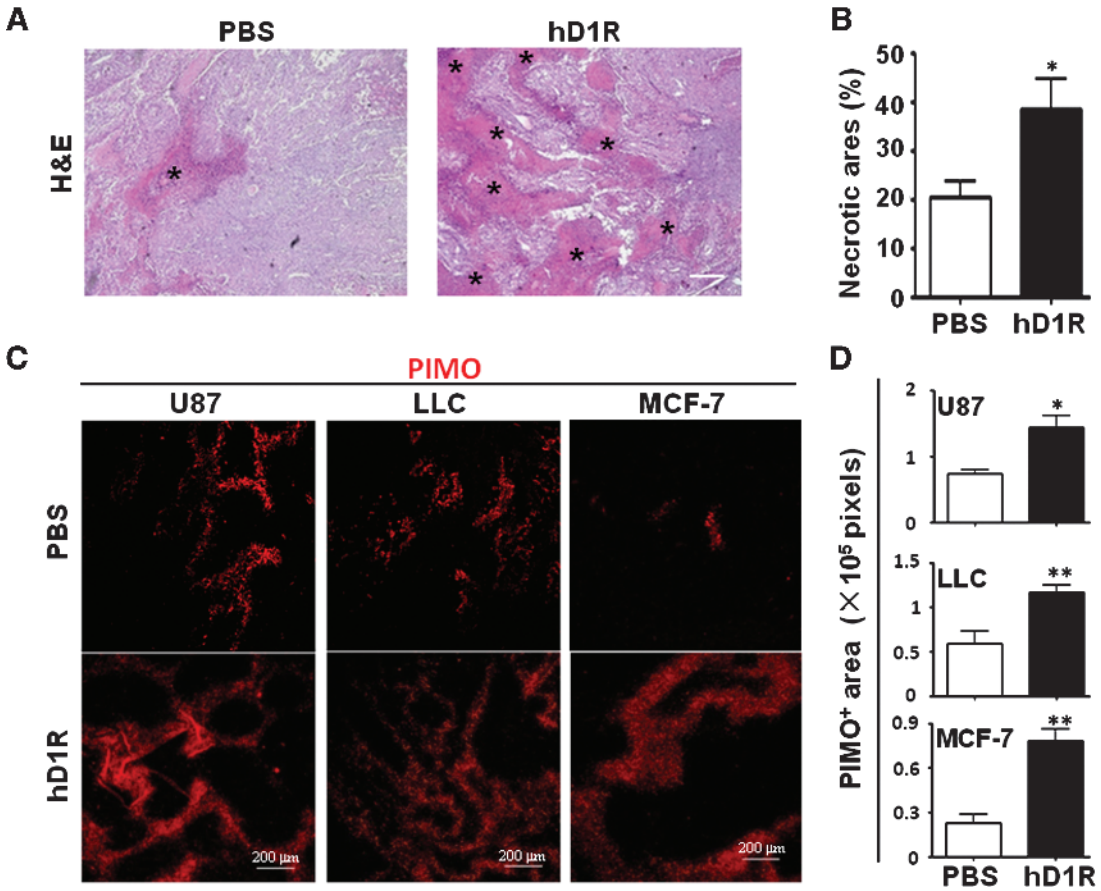

Figure 4. hD1R enhanced tumor hypoxia. (A, B) Tumors were dissected on the ending day of the experiments and subjected to H&E staining (A). Necrosis areas were compared (B). Data from U87 inoculated nude mice were shown. The necrotic areas are marked by asterisks. (C, D) On the last day of the experiments, mice in A were injected i.p. with PIMO and were sacrificed 1 hour later. Tumors of the PBS and hD1R groups were dissected, sectioned, and stained with anti-PIMO (C). $PIMO^+$ (hypoxic) areas per field were quantified and compared (D). Bars, means ± SD. $^*P < .05$, $^{**}P < .01$, $n = 8$.

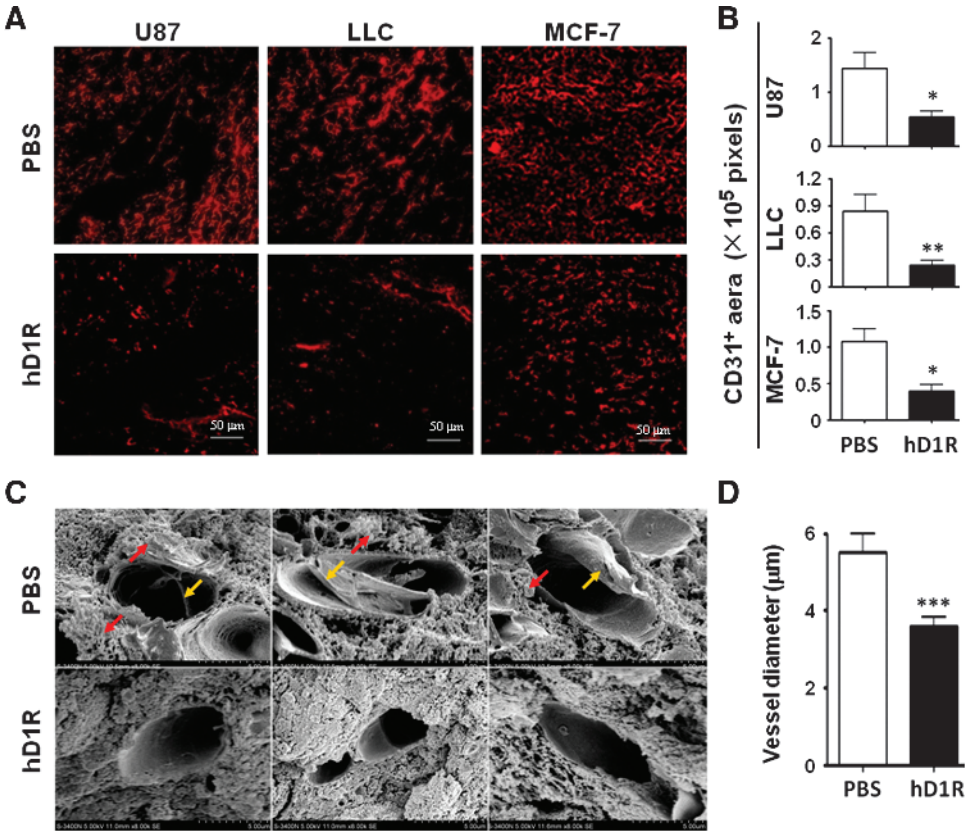

Figure 5. hD1R reduced tumor vasculature. (A, B) U87, LLC, and MCF-7 cells were inoculated s.c. in nude mice. The mice were injected i.p. with PBS or hD1R twice a week from the 7th day of the tumor inoculation. Tumors were dissected on the last day of the experiments, sectioned, and immunostained with anti-CD31. $CD31^+$ areas per field were quantified and were compared between groups (B). (C, D) U87 tumors in A were dissected, sectioned, and observed under SEM (original magnification, × 8000). The yellow arrows and red arrows indicate fibrous materials and leakage-like materials within and outside the microvessels. The shortest inside diameter of each vessel section (20 vessels for each group) was measured and compared (D). Bars, means ± SD. $*P < .05$, $**P < .01$, $***P < .001$, $n = 8$.

showed that there were increased PIMO staining signals in all three types of tumors, indicating enhanced tissue hypoxia in the tumors in mice treated with hD1R (Figure 4, *C* and *D*). These data indicated that hD1R could repress the growth of solid tumors probably through increasing hypoxia in tumor tissues.

hD1R Inhibited Neovascularization of Solid Tumors

We next assessed tumor neovasculature in the hD1R-treated tumor-bearing mice. Tumors were collected from the tumor-bearing mice treated with PBS or hD1R as above. The density of tumor vasculature was evaluated by immunofluorescent staining with anti-CD31. The result showed that the treatment with hD1R significantly reduced vascular density in all three types of tumors (Figure 5, *A* and *B*). The tumor tissues were also co-stained with anti-CD31 and anti–S-Tag antibodies, and the result showed that some of the $S\text{-}Tag^+$ signals overlapped with the $CD31^+$ signal, suggesting that the S-tagged hD1R could bind to ECs in tumors (Figure W7). Collectively, these results indicated that hD1R could reduce tumor neovasculature, most likely through repressing angiogenic sprouting.

We also inspected the structure of tumor vasculature after treatment with hD1R. Under an SEM, the diameter of vessel lumens of the hD1R-treated tumors was reduced (Figure 5, *C* and *D*), possibly due to reduced EC proliferation. Moreover, there were fibrous materials (Figure 5*C*, yellow arrows) and leakage-like materials (Figure 5*C*, red arrows) within and out of microvessels in the control, and these changes were significantly attenuated in the hD1R-treated group, suggesting that the structure of the hD1R-treated tumor vessels might be normalized compared with the controls.

hD1R Enhanced Recruitment of NG2+ Perivascular Cells

Notch signaling could regulate vessel maturation by recruiting perivascular cells including smooth muscle cells (SMCs) and pericytes [38–42]; therefore, we co-stained the tumor sections with anti-NG2 and anti-CD31. The results showed that the hD1R treatment increased $NG2^+$ signals in both LLC and U87 tumors (Figures 6, *A–C*, and W8, *A–C*), suggesting that hD1R treatment promoted the maturation of tumor neovasculatures while reducing the amount of tumor vessels. We then examined the function of tumor vasculature after treatment with hD1R. The tumor-bearing mice treated with PBS or hD1R were injected intravenously with biotinylated lectin before being sacrificed, and the tumor sections were co-stained with streptavidin and anti-CD31. The result showed that the vessel density was reduced, while vessel perfusion was improved in tumors of mice treated with hD1R (Figures 6, *D* and *E*, and W8, *D* and *E*). These results suggested that hD1R might improve tumor vessel integrity, which has been shown to be damaged and results in vessel leakage in tumors.

Discussion

Although it has been revealed that both blocking [13–16,20–24] and activating [19,26–29] Notch signaling result in the disruption of angiogenesis, therapies targeting Notch pathway remain to be established. Because blocking Notch signaling leads to vascular neoplasms [25], activating Notch signaling might be an alternative choice. EC-specific, high efficient activation of Notch signaling, however, is impeded by the facts that Notch ligands are membrane proteins and the activation of Notch receptors requires ligand-mediated endocytosis [30,31]. In this study, to overcome these obstacles, we tried to develop a novel soluble Notch ligand, hD1R, in which the receptor-triggering DSL domain of hDll1 was fused with an EC-targeting peptide RGD. hD1R did not directly influence tumor cell proliferation *in vitro* (data not shown). To interfere with tumor angiogenesis, hD1R has the following advantages. First, it is *in vivo* deliverable as hD1R can be manufactured in *E. coli* in a soluble form and can be administrated by injection. Second, it is EC-targeted because the RGD motif binds to several types of integrins, some of which are expressed on ECs in response to angiogenic growth factors and tumors [32–35]. This may help restrict Notch activation within ECs and other EC-neighboring cells such as blood cells and some stem cells. Indeed, by using a mouse counterpart of hD1R, we found that administration of the recombinant protein *in vivo* did not affect the morphology of main organs (data not shown) nor lymphocyte differentiation and homeostasis [22,43] (Figure W9). Third, hD1R exhibits a strong Notch-activating activity given that RGD motif of hD1R not only provided EC-specific binding capacity but also triggered endocytosis, a process that is essential to Notch activation [30,31]. hD1R could therefore be used to activate endothelial Notch signaling *in vivo* to inhibit angiogenesis in tumors. Moreover, hD1R could also be used to repress angiogenesis in other angiogenic diseases such as age-related macular degeneration [44,45], although an influence on physiological angiogenesis could not be avoided because RGD also targets normal vessels.

Administration of hD1R *in vivo* delays tumor growth and reduces tumor neovascularization most likely through blocking angiogenic sprouting. hD1R may also influence other aspects of tumor angiogenesis including repressing VEGFR2 expression and decreasing EC proliferation, thus reducing the diameter of vessel lumens. Moreover, the hD1R-treated tumor vessels appeared to be better perfused, likely due to improved vessel integrity. This could be helpful for other chemotherapeutics to access tumor cells because a "normalized" vessel structure might inhibit metastasis [46,47], as reported in the study of heterozygous deficiency of PHD2 [48]. Indeed, we observed an additive effect when hD1R was applied together with ChT in MCF7 xenograft tumor models.

Different Notch ligands show distinct even opposing effects on angiogenesis [49,50], which is in line with the observed different roles of hD1R here from reported Dll4 function before. Segarra et al. reported that Dll4-mediated activation of Notch signaling reduced tumor vascularity and inhibits tumor growth [26]. However, Li et al. found that Dll4 reduced the number of tumor blood vessels but improved tumor vascular function [19]. These authors also found that overexpression of Dll4 on tumor cells promoted tumor growth and mediated tumor resistance to anti-VEGF therapy [51]. In contrast, we have shown that the overexpression of Dll1 in tumor cells leads

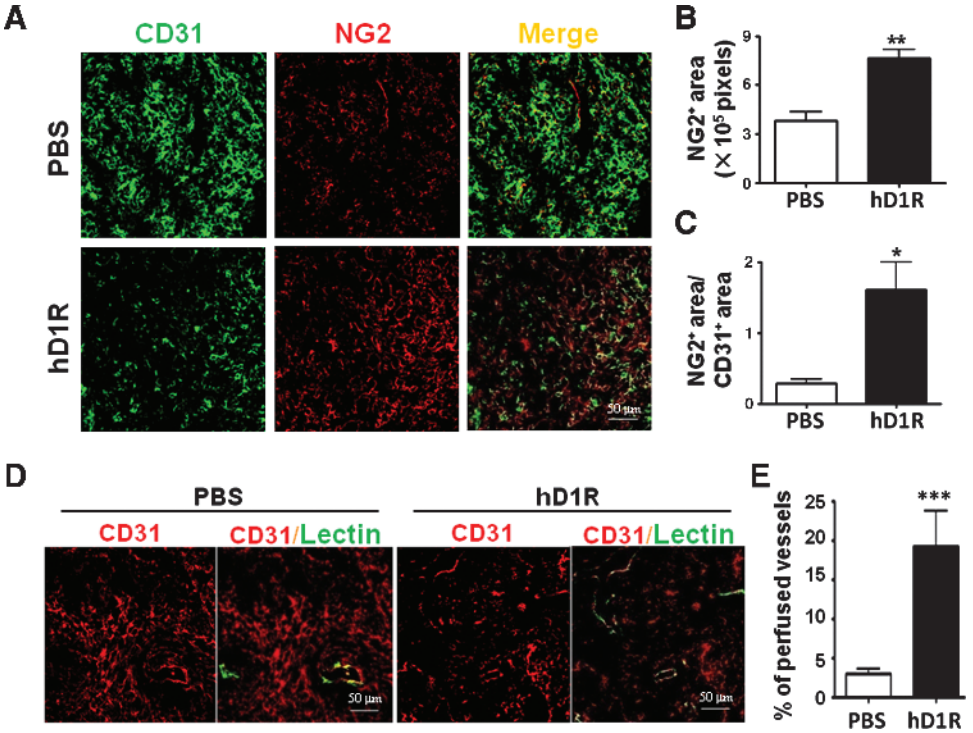

Figure 6. hD1R enhanced the recruitment of perivascular cells. U87 cells were inoculated s.c. in nude mice, and the mice were treated with PBS or hD1R. (A–C) Tumors were stained with anti-CD31 (green) and anti-NG2 (red). The $NG2^+$ areas (B) and the ratio of $NG2^+$ areas *versus* $CD31^+$ areas (C) were compared. (D, E) On the last day of the experiments, mice were injected with lectin (green) through the tail vein. Tumors were dissected 30 minutes after the injection and were stained with anti-CD31 (red). The percentage of the perfused vessels (lectin and CD31 double positive) was counted and compared (E). Bars, means ± SD. $^*P < .05$, $^{**}P < .01$, $^{***}P < .001$, $n = 8$.

to reduced tumor growth attributable to attenuated vascularization [29]. The discrepancy could result from the fact that individual ligands are expressed in different endothelial territories and interact with different Notch receptors following temporospacial-specific patterns during angiogenesis [49]. However, hD1R is a diffusable molecule that may effect on different steps of angiogenesis independent of temporospacial distribution, resulting in reduced vessel formation and better perfusion in tumors.

References

[1] Folkman J (1971). Tumor angiogenesis: therapeutic implications. *N Engl J Med* **285**, 1182–1186.

[2] Folkman J (2003). Fundamental concepts of the angiogenic process. *Curr Mol Med* **3**, 643–651.

[3] Chung AS, Lee J, and Ferrara N (2010). Targeting the tumour vasculature: insights from physiological angiogenesis. *Nat Rev Cancer* **10**, 505–514.

[4] Hurwitz H, Fehrenbacher L, Novotny W, Cartwright T, Hainsworth J, Heim W, Berlin J, Baron A, Griffing S, Holmgren E, et al. (2004). Bevacizumab plus irinotecan, fluorouracil, and leucovorin for metastatic colorectal cancer. *N Engl J Med* **350**, 2335–2342.

[5] Cabebe E and Wakelee H (2006). Sunitinib: a newly approved small-molecule inhibitor of angiogenesis. *Drugs Today (Barc)* **42**, 387–398.

[6] Gerber HP and Ferrara N (2005). Pharmacology and pharmacodynamics of bevacizumab as monotherapy or in combination with cytotoxic therapy in preclinical studies. *Cancer Res* **65**, 671–680.

[7] Siu LL, Awada A, Takimoto CH, Piccart M, Schwartz B, Giannaris T, Lathia C, Petrenciuc O, and Moore MJ (2006). Phase I trial of sorafenib and gemcitabine in advanced solid tumors with an expanded cohort in advanced pancreatic cancer. *Clin Cancer Res* **12**, 144–151.

[8] Casanovas O, Hicklin DJ, Bergers G, and Hanahan D (2005). Drug resistance by evasion of antiangiogenic targeting of VEGF signaling in late-stage pancreatic islet tumors. *Cancer Cell* **8**, 299–309.

[9] Ebos JM, Lee CR, and Kerbel RS (2009). Tumor and host-mediated pathways of resistance and disease progression in response to antiangiogenic therapy. *Clin Cancer Res* **15**, 5020–5025.

[10] Jain RK, Duda DG, Clark JW, and Loeffler JS (2006). Lessons from phase III clinical trials on anti-VEGF therapy for cancer. *Nat Clin Pract Oncol* **3**, 24–40.

[11] Gridley T (2010). Notch signaling in the vasculature. *Curr Top Dev Biol* **92**, 277–309.

[12] Phng LK and Gerhardt H (2009). Angiogenesis: a team effort coordinated by notch. *Dev Cell* **16**, 196–208.

[13] Hellstrom M, Phng LK, Hofmann JJ, Wallgard E, Coultas L, Lindblom P, Alva J, Nilsson AK, Karlsson L, Gaiano N, et al. (2007). Dll4 signalling through Notch1 regulates formation of tip cells during angiogenesis. *Nature* **445**, 776–780.

[14] Lobov IB, Renard RA, Papadopoulos N, Gale NW, Thurston G, Yancopoulos GD, and Wiegand SJ (2007). Delta-like ligand 4 (Dll4) is induced by VEGF as a negative regulator of angiogenic sprouting. *Proc Natl Acad Sci USA* **104**, 3219–3224.

[15] Scehnet JS, Jiang W, Kumar SR, Krasnoperov V, Trindade A, Benedito R, Djokovic D, Borges C, Ley EJ, Duarte A, et al. (2007). Inhibition of Dll4-mediated signaling induces proliferation of immature vessels and results in poor tissue perfusion. *Blood* **109**, 4753–4760.

[16] Suchting S, Freitas C, le Noble F, Benedito R, Breant C, Duarte A, and Eichmann A (2007). The Notch ligand Delta-like 4 negatively regulates endothelial tip cell formation and vessel branching. *Proc Natl Acad Sci USA* **104**, 3225–3230.

[17] Artavanis-Tsakonas S, Rand MD, and Lake RJ (1999). Notch signaling: cell fate control and signal integration in development. *Science* **284**, 770–776.

[18] Zeng Q, Li S, Chepeha DB, Giordano TJ, Li J, Zhang H, Polverini PJ, Nor J, Kitajewski J, and Wang CY (2005). Crosstalk between tumor and endothelial cells promotes tumor angiogenesis by MAPK activation of Notch signaling. *Cancer Cell* **8**, 13–23.

[19] Li JL, Sainson RC, Shi W, Leek R, Harrington LS, Preusser M, Biswas S, Turley H, Heikamp E, Hainfellner JA, et al. (2007). Delta-like 4 Notch ligand regulates tumor angiogenesis, improves tumor vascular function, and promotes tumor growth *in vivo*. *Cancer Res* **67**, 11244–11253.

[20] Noguera-Troise I, Daly C, Papadopoulos NJ, Coetzee S, Boland P, Gale NW, Lin HC, Yancopoulos GD, and Thurston G (2006). Blockade of Dll4 inhibits tumour growth by promoting non-productive angiogenesis. *Nature* **444**, 1032–1037.

[21] Rehman AO and Wang CY (2006). Notch signaling in the regulation of tumor angiogenesis. *Trends Cell Biol* **16**, 293–300.

[22] Ridgway J, Zhang G, Wu Y, Stawicki S, Liang WC, Chanthery Y, Kowalski J, Watts RJ, Callahan C, Kasman I, et al. (2006). Inhibition of Dll4 signalling inhibits tumour growth by deregulating angiogenesis. *Nature* **444**, 1083–1087.

[23] Dufraine J, Funahashi Y, and Kitajewski J (2008). Notch signaling regulates tumor angiogenesis by diverse mechanisms. *Oncogene* **27**, 5132–5137.

[24] Sainson RC and Harris AL (2007). Anti-Dll4 therapy: can we block tumour growth by increasing angiogenesis? *Trends Mol Med* **13**, 389–395.

[25] Yan M, Callahan CA, Beyer JC, Allamneni KP, Zhang G, Ridgway JB, Niessen K, and Plowman GD (2010). Chronic DLL4 blockade induces vascular neoplasms. *Nature* **463**, E6–E7.

[26] Segarra M, Williams CK, Sierra Mde L, Bernardo M, McCormick PJ, Maric D, Regino C, Choyke P, and Tosato G (2008). Dll4 activation of Notch signaling reduces tumor vascularity and inhibits tumor growth. *Blood* **112**, 1904–1911.

[27] Trindade A, Kumar SR, Scehnet JS, Lopes-da-Costa L, Becker J, Jiang W, Liu R, Gill PS, and Duarte A (2008). Overexpression of delta-like 4 induces arterialization and attenuates vessel formation in developing mouse embryos. *Blood* **112**, 1720–1729.

[28] Williams CK, Li JL, Murga M, Harris AL, and Tosato G (2006). Up-regulation of the Notch ligand Delta-like 4 inhibits VEGF-induced endothelial cell function. *Blood* **107**, 931–939.

[29] Zhang JP, Qin HY, Wang L, Liang L, Zhao XC, Cai WX, Wei YN, Wang CM, and Han H (2011). Overexpression of Notch ligand Dll1 in B16 melanoma cells leads to reduced tumor growth due to attenuated vascularization. *Cancer Lett* **309**, 220–227.

[30] Fortini ME and Bilder D (2009). Endocytic regulation of Notch signaling. *Curr Opin Genet Dev* **19**, 323–328.

[31] Seugnet L, Simpson P, and Haenlin M (1997). Requirement for dynamin during Notch signaling in *Drosophila* neurogenesis. *Dev Biol* **192**, 585–598.

[32] Avraamides CJ, Garmy-Susini B, and Varner JA (2008). Integrins in angiogenesis and lymphangiogenesis. *Nat Rev Cancer* **8**, 604–617.

[33] Spitaleri A, Mari S, Curnis F, Traversari C, Longhi R, Bordignon C, Corti A, Rizzardi GP, and Musco G (2008). Structural basis for the interaction of *iso*DGR with the RGD-binding site of αvβ3 integrin. *J Biol Chem* **283**, 19757–19768.

[34] McDonald DM and Choyke PL (2003). Imaging of angiogenesis: from microscope to clinic. *Nat Med* **9**, 713–725.

[35] Caswell PT, Vadrevu S, and Norman JC (2009). Integrins: masters and slaves of endocytic transport. *Nat Rev Mol Cell Biol* **10**, 843–853.

[36] Nakatsu MN, Sainson RC, Aoto JN, Taylor KL, Aitkenhead M, Perez-del-Pulgar S, Carpenter PM, and Hughes CC (2003). Angiogenic sprouting and capillary lumen formation modeled by human umbilical vein endothelial cells (HUVEC) in fibrin gels: the role of fibroblasts and Angiopoietin-1. *Microvasc Res* **66**, 102–112.

[37] Dou GR, Wang YC, Hu XB, Hou LH, Wang CM, Xu JF, Wang YS, Liang YM, Yao LB, Yang AG, et al. (2008). RBP-J, the transcription factor downstream of Notch receptors, is essential for the maintenance of vascular homeostasis in adult mice. *FASEB J* **22**, 1606–1617.

[38] Regan JN and Majesky MW (2009). Building a vessel wall with notch signaling. *Circ Res* **104**, 419–421.

[39] Stewart KS, Zhou Z, Zweidler-McKay P, and Kleinerman ES (2011). Delta-like ligand 4–Notch signaling regulates bone marrow–derived pericyte/vascular smooth muscle cell formation. *Blood* **117**, 719–726.

[40] Liu H, Kennard S, and Lilly B (2009). NOTCH3 expression is induced in mural cells through an autoregulatory loop that requires endothelial-expressed JAGGED1. *Circ Res* **104**, 466–475.

[41] Jin S, Hansson EM, Tikka S, Lanner F, Sahlgren C, Farnebo F, Baumann M, Kalimo H, and Lendahl U (2008). Notch signaling regulates platelet-derived growth factor receptor-β expression in vascular smooth muscle cells. *Circ Res* **102**, 1483–1491.

[42] Liu H, Zhang W, Kennard S, Caldwell RB, and Lilly B (2010). Notch3 is critical for proper angiogenesis and mural cell investment. *Circ Res* **107**, 860–870.

[43] Wu Y, Cain-Hom C, Choy L, Hagenbeek TJ, de Leon GP, Chen Y, Finkle D, Venook R, Wu X, Ridgway J, et al. (2010). Therapeutic antibody targeting of individual Notch receptors. *Nature* **464**, 1052–1057.

[44] Dou GR, Wang L, Wang YS, and Han H (2012). Notch signaling in ocular vasculature development and diseases. *Mol Med* **18**, 47–55.

[45] Chiang A and Regillo CD (2011). Preferred therapies for neovascular age-related macular degeneration. *Curr Opin Ophthalmol* **22**, 199–204.

[46] Carmeliet P and Jain RK (2011). Principles and mechanisms of vessel normalization for cancer and other angiogenic diseases. *Nat Rev Drug Discov* **10**, 417–427.

[47] Goel S, Duda DG, Xu L, Munn LL, Boucher Y, Fukumura D, and Jain RK (2011). Normalization of the vasculature for treatment of cancer and other diseases. *Physiol Rev* **91**, 1071–1121.

[48] Mazzone M, Dettori D, Leite de Oliveira R, Loges S, Schmidt T, Jonckx B, Tian YM, Lanahan AA, Pollard P, Ruiz de Almodovar C, et al. (2009). Heterozygous deficiency of PHD2 restores tumor oxygenation and inhibits metastasis via endothelial normalization. *Cell* **136**, 839–851.

[49] Benedito R, Roca C, Sorensen I, Adams S, Gossler A, Fruttiger M, and Adams RH (2009). The notch ligands Dll4 and Jagged1 have opposing effects on angiogenesis. *Cell* **137**, 1124–1135.

[50] Trifonova R, Small D, Kacer D, Kovalenko D, Kolev V, Mandinova A, Soldi R, Liaw L, Prudovsky I, and Maciag T (2004). The non-transmembrane form of Delta1, but not of Jagged1, induces normal migratory behavior accompanied by fibroblast growth factor receptor 1-dependent transformation. *J Biol Chem* **279**, 13285–13288.

[51] Li JL, Sainson RC, Oon CE, Turley H, Leek R, Sheldon H, Bridges E, Shi W, Snell C, Bowden ET, et al. (2011). DLL4-Notch signaling mediates tumor resistance to anti-VEGF therapy *in vivo*. *Cancer Res* **71**, 6073–6083.

Table W1. Primers Used in This Study.

Gene	Purpose	Direction	Sequence
Human β-actin	RT-PCR	Forward	5′-TGGCACCCAGCACAATGAA
		Backward	5′-CTAAGTCATAGTCCGCCTAGAAGCA
Human Hes1	RT-PCR	Forward	5′-TGGAAATGACAGTGAAGCACCTC
		Backward	5′-TCGTTCATGCACTCGCTGAAG
Human Hey1	RT-PCR	Forward	5′-CATGAAGAGAGCTCACCCAGA
		Backward	5′-CGCCGAACTCAAGTTTCC
Mouse β-actin	RT-PCR	Forward	5′-CATCCGTAAAGACCTCTATGCCAAC
		Backward	5′-ATGGAGCCACCGATCCACA
Mouse Hes1	RT-PCR	Forward	5′-AAAGACGGCCTCTGAGCAC
		Backward	5′-GGTGCTTCACAGTCATTTCCA
Mouse VEGFR1	RT-PCR	Forward	5′-TAATGACGATGGCAACAGGGTAGA
		Backward	5′-TGTGCACGACCTAAGCACACAG
Mouse VEGFR2	RT-PCR	Forward	5′-GGGATGGTCCTTGCATCAGAA
		Backward	5′-ACTGGTAGCCACTGGTCTGGTTG
hD1S	Cloning	Forward	5′-CGCCATGGTCCACACAGATTCTCCTG
		Backward	5′-CGCTCGAGGATCGGCTCTGTGCAGTAG
hD1D	Cloning	Forward	5′-CGCCATGGTCCACACAGATTCTCCTG
		Backward	5′-CGCTCGAGTTAGTATCTAACGCCGCATCTGCCATCGCAGATCGGCTCTGTGCAGTAG
hD1R	Cloning	Forward	5′-CGCCATGGTCCACACAGATTCTCCTG
		Backward	5′-CGCTCGAGTTAGTATCTAACGCCGCAATCGCCTCTGCAGATCGGCTCTGTGCAGTAG

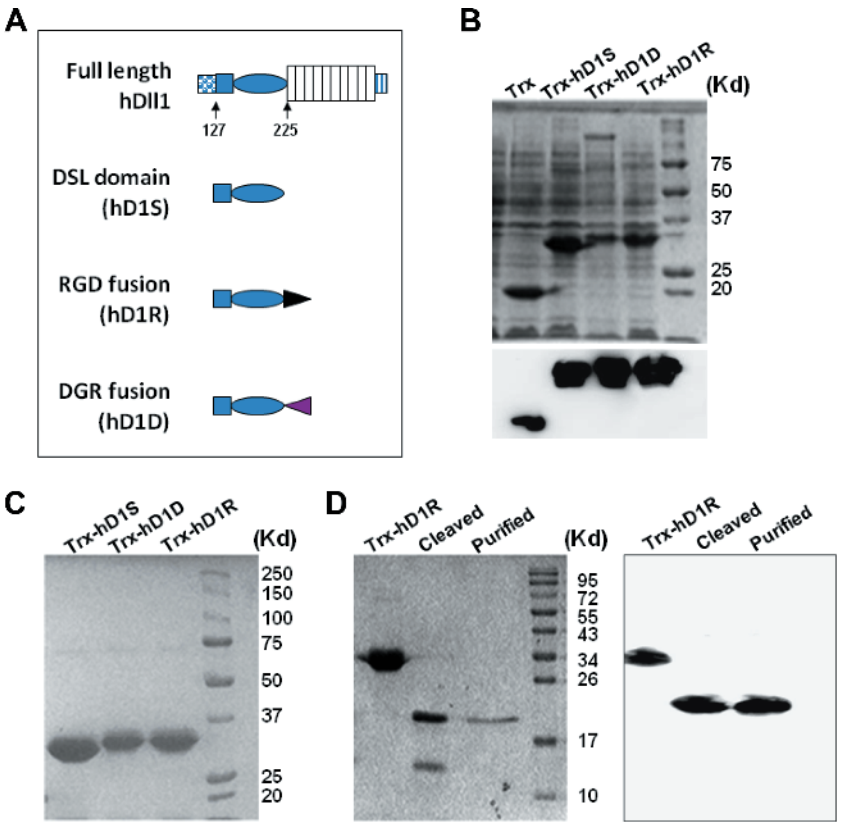

Figure W1. Expression of hD1R, an EC-targeted DSL domain of hDll1. (A) Schematic illustrations of the full-length hDll1, the DSL domain of hDll1 (hD1S), hDll1 fused with the RGD peptide (hD1R), and hDll1 fused with the DGR peptide (hD1D). (B) *E. coli* (BL21) was transformed with pET32(a), pET32a-hD1S, pET32a-hD1D, or pET32a-hD1R. Positive transformants were induced with isopropyl β-D-thiogalactoside. Total cell lysates were analyzed by SDS-PAGE (upper). The gel was blotted onto PVDF membrane and probed with the anti-His antibody (lower). (C) The recombinant Trx-hD1S, Trx-hD1D, and Trx-hD1R proteins were purified with Ni^{+}-NTA columns and analyzed by using SDS-PAGE. (D) Trx-hD1R was cleaved with thrombin and purified by using an Ni^{+}-NTA column. The eluent was analyzed by SDS-PAGE (left), followed by Western blot by using anti–S-Tag.

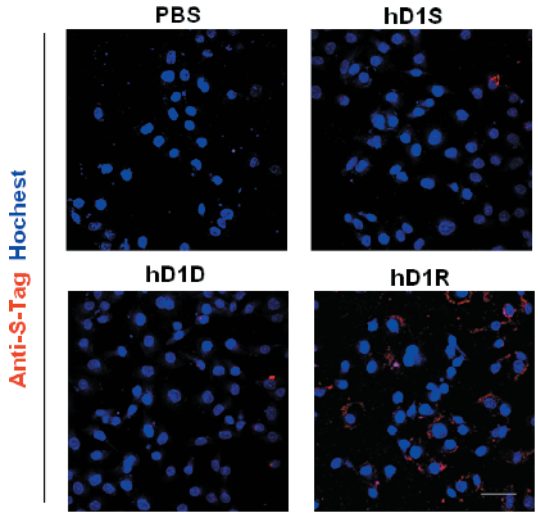

Figure W2. hD1R could efficiently bind to ECs. HUVECs were incubated with PBS, hD1S, hD1D, or hD1R for 2 hours. Cells were washed with PBS and fixed with 4% paraformaldehyde. Samples were then stained with anti–S-Tag plus Cy3-conjugated secondary antibody and observed under a confocal microscope.

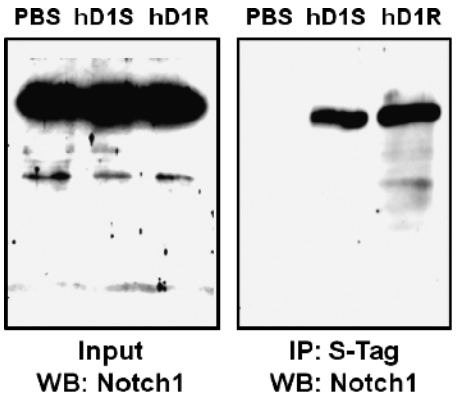

Figure W4. hD1S and hD1R could interact with the extracellular domain of Notch1 receptor. HUVECs were lysed with cell lysis buffer, and the supernatants were incubated with PBS, hD1S, or hD1R. Immunoprecipitation was performed with anti–S-Tag, and the presence of Notch1 extracellular domain was detected by immunoblot analysis with anti-Notch1. For methodology, HUVECs were washed once with ice-cold PBS and lysed in IP buffer (Beyotime, Haimen, China). Cell lysates were incubated with PBS, S-tagged hD1S, or S-tagged hD1R for 2 hours at 4°C and then incubated with protein G-Sepharose beads (Invitrogen) precoated with anti–S-Tag antibody (1:200; Abcam) overnight. The beads were washed extensively, and co-precipitated proteins were detected by immunoblot analysis with an anti-Notch1 (Santa Cruz Biotechnology, Inc) as the primary antibody.

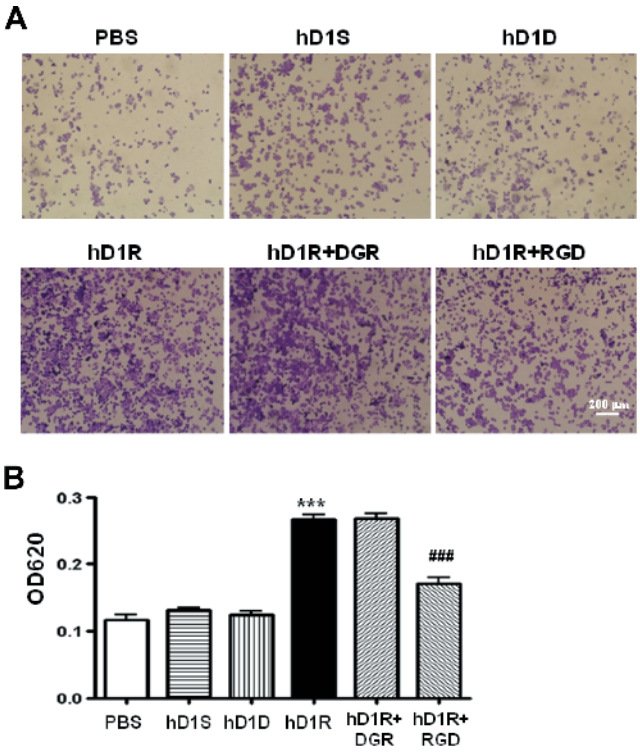

Figure W3. hD1R bound to ECs through the RGD motif. (A) Culture dishes were coated with PBS, hD1S, hD1D, or hD1R. HUVECs were distributed into different wells and incubated for 1.5 hours. In some wells, synthetic DGR or RGD nonapeptide was included. After incubation, wells were washed with medium and nonadherent cells were discarded. Adherent cells were stained with crystal violet and photographed. (B) Cells in A were lysed, and A620 in the supernatants was detected and compared between different groups. Bars, means ± SD. $^{***, ###}P < .001$, $n = 4$.

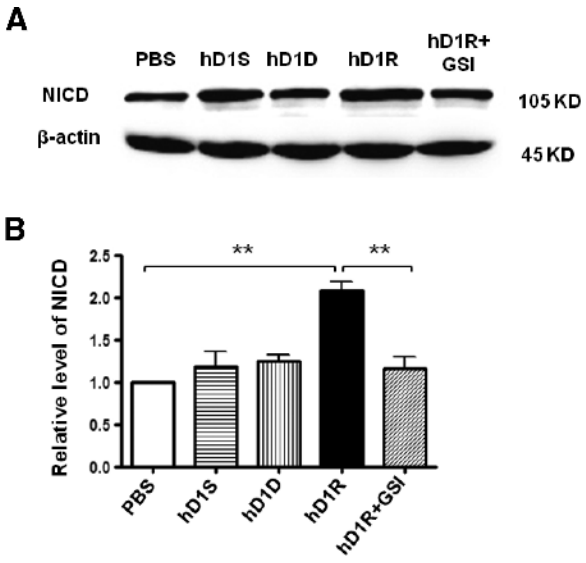

Figure W5. Western blot. (A) HUVECs were incubated with PBS, hD1S, hD1D, or hD1R for 24 hours. GSI was included in some of the cultures as indicated. Total cell lysates were prepared and analyzed by SDS-PAGE. The gel was blotted onto PVDF membrane and probed with the anti-NICD antibody, with β-actin as an internal control. (B) Each band was quantified by grayscale scanning, and the relative level of NICD was compared. Bars, means ± SD. $^{**}P < .01$, $n = 3$.

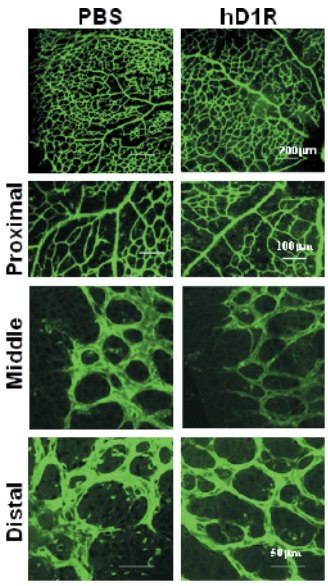

Figure W6. hD1R repressed angiogenesis *in vivo*. P3 pups were injected daily s.c. with PBS or hD1R. On P7, the retinas of the pups were collected, flat-mounted, and stained with fluorescein-labeled *Griffonia simplicifolia* Lectin I. The structures of the whole retinal vasculature and the proximal, middle, and distal areas were shown.

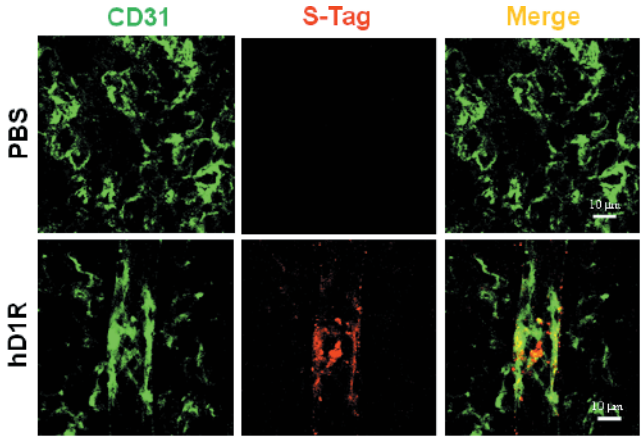

Figure W7. hD1R bound to tumor vessels *in vivo*. Nude mice were inoculated s.c. with U87 glioma cells (5×10^6) on the back. Mice were injected i.p. with PBS or hD1R twice a week from the 7th day of inoculation. At the ending day of the experiments, the tumors were dissected 30 minutes after the last injection, sectioned, and stained by using anti-CD31 (green) and anti–S-Tag (red).

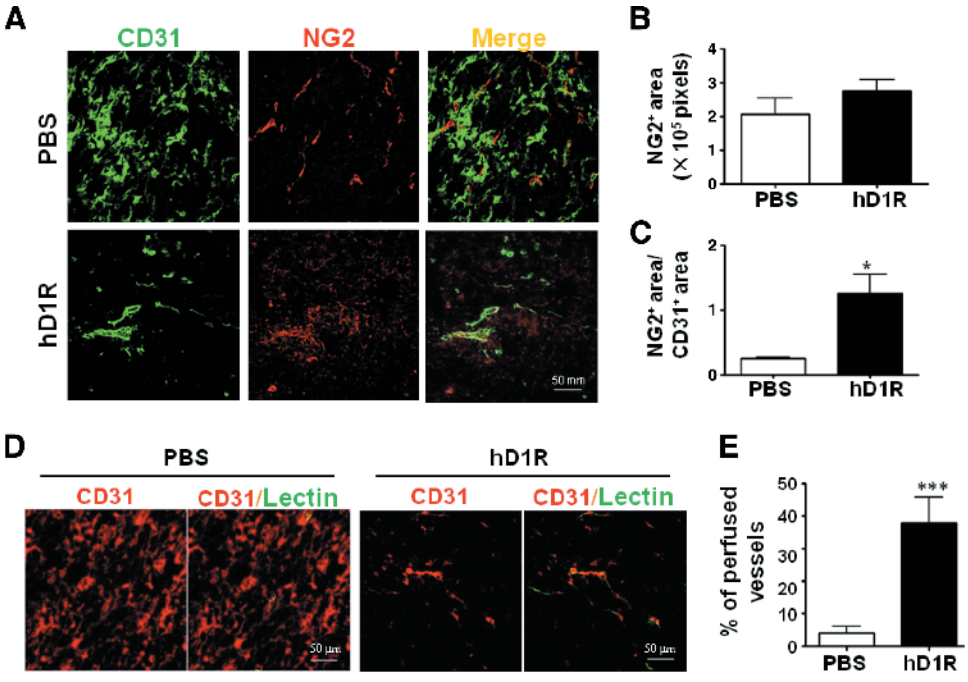

Figure W8. hD1R enhanced the recruitment of perivascular cells. LLC cells were inoculated s.c. in nude mice, and the mice were treated with PBS or hD1R. (A–C) Tumors were stained with anti-CD31 (green) and anti-NG2 (red). The $NG2^+$ areas (B) and the ratio of $NG2^+$ areas *versus* $CD31^+$ areas (C) were compared. (D, E) On the last day of the experiments, mice were injected with lectin (green) through the tail vein. Tumors were dissected 30 minutes after the injection and were stained with anti-CD31 (red). The percentage of the perfused vessels (lectin and CD31 double positive) was counted and compared (E). Bars, means ± SD. $^*P < .05$, $^{***}P < .001$, $n = 8$.

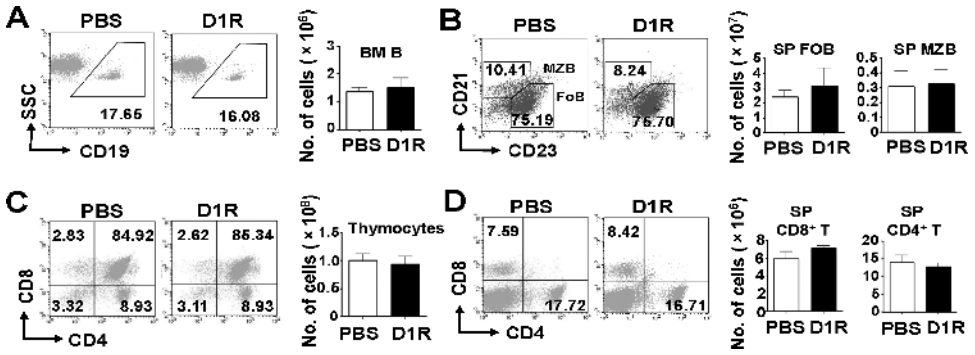

Figure W9. mD1R did not affect lymphocyte differentiation and homeostasis. Mice were injected i.p. with PBS or mD1R twice a week for 4 weeks. On day 28 after treatment, lymphoid organs were collected. Single-cell suspensions were prepared and analyzed by flow cytometry with the indicated staining settings. (A) Bone marrow (BM) B cell analysis shown by representative $CD19^+$ B cell FACS plots along with cell numbers on the side. (B) Spleen follicular (Fo) B and marginal zone (MZ) B cell distribution displayed by B220CD21CD23 profiles of splenocytes. (C) Thymocyte subset analysis shown by CD4CD8 profiles of thymocytes. (D) Spleen T cell subset analysis presented by CD4CD8 profiles of splenocytes. Bars, mean ± S.D. $n = 5$.